Received: 6 March 2019 | Accepted: 5 July 2019 | Published online: 10 January 2020

DOI: 10.1002/agj2.20043

Agronomy Journal

ARTICLE

Biometry, Modeling, & Statistics

Modelling root water uptake under deficit irrigation and rewetting in Northwest China

Xiaowen Wang[1,2,3] | **Huanjie Cai**[1,2,3] | **Zhen Zheng**[4] | **Lianyu Yu**[5] | **Zishen Wang**[6] | **Liang Li**[1,2,3]

[1]Key Lab. of Agricultural Soil and Water Engineering in Arid and Semiarid Areas, Ministry of Education, Northwest A&F Univ., Yangling, Shaanxi, 712100, China

[2]Institute of Water-saving Agriculture in Arid Areas of China, Northwest A&F Univ., Yangling, Shaanxi, 712100, China

[3]College of Water Resources and Architectural Engineering, Northwest A&F Univ., Yangling, Shaanxi, 712100, China

[4]Research Center of Fluid Machinery Engineering and Technology, Jiangsu Univ., Zhenjiang 212013, China

[5]Faculty of Geo-information and Earth Observation (ITC), Univ. of Twente, Enschede 7514AE, Netherlands

[6]Centre for Crop Systems Analysis (CSA) Wageningen Univ. & Research, Wageningen 6708PB, Netherlands

Correspondence
Huanjie Cai, Key Lab. of Agricultural Soil and Water Engineering in Arid and Semiarid Areas, Ministry of Education, Northwest A&F Univ., Yangling, Shaanxi, 712100, China.
Email: huanjiec@yahoo.com

Funding information
National Key Research and Development Program of China, Grant/Award Number: 2016YFC0400200; National Natural Science Foundation of China, Grant/Award Number: 51879223

Abstract

The spatial and temporal distribution of root water uptake (RWU) under deficit irrigation are critical factors for crop growth. The SWAP (soil–water–atmosphere–plant) model was applied to analyze the pattern of RWU for winter wheat (*Triticum aestivum* L.) under three irrigation levels: no water deficit (100% evapotranspiration [ET]), moderate water deficit (80% ET) and severe water deficit (60% ET). The 2–yr experiments indicated that SWAP was highly accurate (mean relative error [MRE] <21.7%, root mean square error [RMSE] <0.07 cm^3 cm^{-3}) in simulating the soil water content (SWC). Root water uptake was significantly ($P < 0.01$) different in the 0- to 60-cm soil layer. The 0- to 60-cm soil layer was the main source of RWU, and the average value accounted for 89.4% of the total root zone. Water stress had the greatest adverse effect on heading to grain filling, reducing RWU by 0.0026 cm^3 cm^{-3} d^{-1}. The critical SWC was 67.9% of the field capacity, when the RWU dropped to 95% of the control treatment. After rewetting, compensation and hysteresis effects on RWU were observed. The ranking of RWU recovery ability after rewetting was: emergence to jointing > jointing to heading > grain filling to maturity > heading to grain filling. Recovery time of RWU was 2 to 11 d and gradually increased with growth stage. The simplified RWU model established using path analysis and regression performed well ($R^2 = 0.836$; $P < 0.01$) for RWU. This provided a more convenient way to accurately estimate RWU with fewer variables.

1 | INTRODUCTION

Water scarcity in northwest China has become a serious challenge as a result of accelerating industrialization, urbanization, and environmental pollution (Tang, Folmer, & Xue, 2015). The Guanzhong Plain is an important grain production

Abbreviations: DC, decision coefficient; ET, evapotranspiration; LAI, leaf area index; MRE, mean relative error; RH, relative humidity; RMSE, root mean square error; RWU, root water uptake; SWAP, soil–water–atmosphere–plant; SWC, soil water content.

area in northwest China. Water consumption due to irrigation in this area accounts for 60% of the total water resources (Tang, Folmer, & Xue, 2016). Winter wheat (*Triticum aestivum* L.) is one of the major food crops in this area. However, the spatial and temporal distribution of precipitation in the Guanzhong Plain is uneven. During the winter wheat growing season (October–June), precipitation is only 130 to 250 mm (Zheng, Cai, Hoogenboom, Chaves, & Yu, 2016). This precipitation is far from meeting the water requirements of winter wheat. Therefore, irrigation is usually required several times throughout the growing season (Guo et al., 2018; Zhang, Pei, & Chen, 2004). Serious water shortages force people to implement deficit irrigation. Researchers have reported that this irrigation method can effectively improve water use efficiency without many adverse effects on yield (Han, Ren, Gao, Yan, & Li, 2017; Li, Bian, Liu, Ma, & Liu, 2015).

Complex crop responses to water stress have continually been a research focus of deficit irrigation (Andarzian et al., 2011; Iqbal et al., 2014; Mkhabela & Bullock, 2012; Steduto, Hsiao, Raes, & Fereres, 2009; Toumi et al., 2016). Many studies have analyzed the relationships between crop growth, ET, and RWU (Goosheh, Pazira, Gholami, Andarzian, & Panahpour, 2018; Han et al., 2017; Jha et al., 2017), while others have studied crop growth and ET under deficit irrigation (Salemi et al., 2011; Yu, Zeng, Su, Cai, & Zheng, 2016). Andarzian et al. (2011), Benabdelouahab et al. (2016) and Mkhabela and Bullock (2012) evaluated the performance of the AquaCrop model for its ability to simulate wheat yield and SWC under different irrigation scenarios. However, little is known about the below surface status. Roots are highly sensitive to water stress (Jha et al., 2017). Root water uptake is an important process for plants because it regulates nutrient transport, water balance, and yield (Cai et al., 2018; Xue, Zhu, Musick, Stewart, & Dusek, 2003). It is almost impossible to select a reasonable water management method without understanding RWU and soil moisture dynamics (Jha et al., 2017). Root water uptake is influenced by characteristics of the crop, soil and meteorology (Cao, Yang, Engel, & Li, 2018). Zhang et al. (2004) found that the root profile distribution determined the main source of water uptake. Research by Xue et al. (2003) showed that RWU decreased from booting to the late grain filling stage due to low SWC. Irrigation methods affected the total RWU from regreening to harvesting (Jha et al., 2017). In addition, atmospheric transpiration potential has often been considered in RWU under stress conditions (Yang et al., 2009).

It is usually difficult to observe the root system completely by sampling. Quantifying RWU in different regions and climatic conditions also remains a challenge because some key parameters of RWU and a proper description for RWU process are often lacking (Vereecken et al., 2016). Many researchers have proposed multiple RWU models based on different principles, which are divided into microscopic and macroscopic models. The microscopic model is based on the study of the radial flow of soil water to a single root (Doussan, Pierret, Garrigues, & Pagès, 2006; Javaux, Schröder, Vanderborght, & Vereecken, 2008). Since parameters are complex and difficult to measure (such as detailed geometry, soil heterogeneity and different water permeability of the roots), microscopic models have not been in widespread use (Babazadeh, Sarai Tabrizi, & Homaee, 2017; Sonkar, Kaushika, & Hari Prasad, 2018). In contrast, macroscopic models (Feddes, Kowalik, Kolinska-Malinka, & Zaradny, 1976; Prasad, 1988; Vrugt, Hopmans, & Simunek, 2001) describe the water motion in the unsaturated zone using the sink term in Richards' equation (Richards, 1931). Macroscopic models do not require complete insight into the biophysical processes of root–soil interactions. Therefore, macroscopic models are more widely used due to their simplicity.

Macroscopic models are also nested in various agro-hydrological models to guide agricultural production through numerical simulations such as SWAP (Eitzinger, Trnka, Hosch, Zalud, & Dubrovsky, 2004; Mostafazadeh-Fard, Mansouri, Mousavi, & Feizi, 2007), Hydrus (Zeng et al., 2018) and MACRO (Bonfante et al., 2010). SWAP has performed well for simulations of farmland water and heat flow under different soil conditions (Martínez-Ferri, Muriel-Fernández, & Díaz, 2013). The SWAP model has also been used to schedule irrigation (Jiang, Feng, Ma, Huo, & Zhang, 2016; Ma, Feng, & Song, 2015; Rallo, Agnese, Minacapilli, & Provenzano, 2012) and estimate crop yield at the field and regional scale (de Jong van Lier, Wendroth, & van Dam, 2015; Hassanli, Ebrahimian, Mohammadi, Rahimi, & Shokouhi, 2016; Mokhtari, Noory, & Vazifedoust, 2018). Some research has shown that SWAP simulation results are superior to other models (Bonfante et al., 2010; Eitzinger et al., 2004; Hassanli et al., 2016). However, not many studies have predicted RWU

Core Ideas

- The SWAP model performed well in simulating soil water content under different irrigation conditions.
- Root water uptake was related to irrigation amount, and the 0–60 cm soil layer was the main source of root uptake.
- Water stress increased uptake in emergence-to-jointing and had a negative impact on uptake at heading-to-grain filling.
- After rewetting, the root water uptake exhibited compensation effect and hysteresis effect.
- Root uptake was well-described by the simplified model using days after emergence, radiation, and soil water (0-60 cm).

based on SWAP. In addition, the numerical model requires multiple input parameters. Many parameters can only be obtained through laboratory tests rather than field observations. This limits the representativeness of the parameters. Parameter adjustment before simulation often requires substantial time and effort. Many researchers (Cai, Vanderborght, Couvreur, Mboh, & Vereecken, 2017; Šimůnek & Hopmans, 2009) have found that certain soil moisture indicators are adequate to infer soil and root properties through reverse modeling. A simplified RWU estimation model can be constructed by optimizing algorithms with few representative parameters.

There are three aims in this winter wheat trial of deficit irrigation: (i) test how measured SWC compares with results simulated by SWAP to determine if the model is suitable for local use, (ii) test how the temporal and spatial distribution characteristics of RWU differ under different soil water conditions, and (iii) based on the simulation results and path analysis, identify the most representative variables affecting RWU to establish a simplified RWU model.

2 | MATERIALS AND METHODS

2.1 | Field experiment

The experiment was performed from October 2012 to June 2014 at the Institute of Water-saving Agriculture in Arid Areas of China (108°04¢ E, 34°17′ N; 521 m above sea level), Northwest A&F University, Yangling, Shaanxi Province, China. The test area is in a semiarid climate zone where the average annual temperature is 12.5°C. The average annual precipitation and potential evaporation are 609 and 1500 mm, respectively. The local soil texture is silty clay loam (Table 1). The average field capacity of 100-cm soil layer is 25% (mass water content), and the average bulk density is 1.36 g cm^{-3}. Groundwater is deep, thus recharge can be disregarded. The plot area is 6.6 m^2 (length 3 m, width 2.2 m and depth 3 m) and a filter layer is placed at the bottom for free drainage. Each plot is separated by concrete (thickness 25 cm) to avoid lateral water leakage. A mobile electric shelter (length 48 m, width 10 m and height 4 m) is installed above the plots to avoid the impact of precipitation on results. The shelter is made of transparent plastic to reduce the shading to crops during closure.

The winter wheat variety was Xiaoyan 22, which is widely cultivated in Shaanxi Province. The seeding rate was 357 million km^{-2}. Each treatment received N (the N fertilizer used was urea) at a rate of 24.4 t km^{-2} and P_2O_5 at a rate of 27.0 t km^{-2} at the time of sowing. The winter wheat was divided into four growth stages: emergence to jointing, jointing to heading, heading to grain filling, and grain filling to maturity (Table 2). Letters W and T indicate treatments of the 2012–2013 and 2013–2014 growing seasons, respectively. Based on actual ET of sufficient irrigation treatments (W1 and T1) measured by a lysimeter, we set three irrigation levels at each stage: no water deficit (100% ET), moderate water deficit (80% ET) and severe water deficit (60% ET). The experiment was designed using an orthogonal test with four factors and three levels. There were nine treatments with three replicates (Table 3).

TABLE 1 Physical properties of the soil (silty clay loam) at the experimental area in Yangling, Shaanxi Province, China

Soil layer	Soil property			
	Sand	Silt	Clay	Bulk density
cm	%			g cm^{-3}
0–23	26.71	50.85	22.10	1.32
23–35	24.98	52.78	22.10	1.40
35–95	22.11	54.75	20.90	1.41
95–196	21.32	48.60	30.10	1.36
196–250	30.64	47.55	21.60	1.32

2.2 | Meteorology, soils, and crop data

Daily weather data were obtained from the Yangling national general weather station with maximum and minimum temperature, relative humidity (RH), 2-m wind speed, sunshine length and precipitation. Soil water content was measured by the weighing dry soil method every 7 to 10 d. From the soil surface down to a depth of 100 cm, every 10-cm layer was sampled. The actual ET was automatically measured by two large weighing lysimeters (New Huize measurement and control technology Co., Ltd, Xi'an, China), which are the same

TABLE 2 Date and duration of each growth stage and irrigation for winter wheat during the 2012 to 2013 and 2013 to 2014 growing seasons

Year	Treatments	Sowing	Emergence to jointing	Jointing to heading	Heading to grain filling	Grain filling to maturity	Harvest
2012–2013	W1–W9	17 Oct. 2012	25 Oct. 2012–14 Mar. 2013 (27 Dec. 2012)[a]	15 Mar. 2013–9 Apr. 2013 (15 Mar. 2013)	10 Apr. 2013–1 May 2013 (11 Apr. 2013)	2 May 2013–3 June 2013 (4 May 2013)	3 June 2013
2013–2014	T1–T9	15 Oct. 2013	24 Oct. 2013–25 Mar. 2014 (28 Dec. 2013)	26 Mar. 2014–19 Apr. 2014 (31 Mar. 2014)	20 Apr. 2014–15 May 2014 (8 May 2014)	16 May 2014–8 June 2014	8 June 2014

[a]Dates of irrigation in parentheses.

TABLE 3 Three irrigation levels based on actual evapotranspiration of full irrigation (W1 and T1) measured by lysimeter during four growth stages of winter wheat in the 2012 to 2013 and 2013 to 2014 growing seasons

		Irrigation quota per growth stage				
		Emergence to jointing	Jointing to heading	Heading to grain filling	Grain filling to maturity	Irrigation norm
Year	Treatment	mm				
2012–2013	W1	82	75	90	90	337
	W2	82	60	72	72	286
	W3	82	45	54	54	235
	W4	67	75	72	54	268
	W5	67	60	54	90	271
	W6	67	45	90	72	274
	W7	52	75	54	72	253
	W8	52	60	90	54	256
	W9	52	45	72	90	259
2013–2014	T1	84	75	105	0	264
	T2	84	60	84	0	228
	T3	84	45	63	0	192
	T4	67	75	63	0	205
	T5	67	60	105	0	232
	T6	67	45	84	0	196
	T7	52	75	84	0	211
	T8	52	60	63	0	175
	T9	52	45	105	0	202

size as the plots. The range of the device was 0 to 6 t, and the measurement accuracy was less than 150 g (Yu et al., 2016). We randomly selected 10 plants every 7 to 10 d to measure crop height using a tapeline with accuracy of 1 mm. Leaf area index (LAI) was measured at each growth stage by a SunScan-SS1 canopy analyzer (Delta-T Devices Ltd, Cambridge, UK).

2.3 | SWAP model

The SWAP v.4 model (Kroes et al., 2017) can simulate the interaction of water, solute, heat, and crop growth in a seepage area using local meteorology, soil and crop data. This model has a strong physical basis known as the one-dimensional Richards' equation (Bonfante et al., 2010). SWAP has been applied widely in different agro-hydrological scenarios (Eitzinger et al., 2004; Hassanli et al., 2016; Jiang et al., 2016; Mokhtari et al., 2018).

2.3.1 | Input module

Meteorological module data came from a weather station near the plot (approximately 0.3 km). The soil module requires discreet horizons. The 0- to 100-cm soil profile was divided into five layers on average with multiple calculation compartments of different thicknesses. This study was focused on the transformation of soil water and crop water use in farmlands, and the simple crop module in the SWAP model was selected (Kroes et al., 2017). This module is based on the concept of a green canopy that intercepts precipitation, transpires water vapor and shades the ground. The crop growth duration was fixed and derived from measured growth dates. Crop variables (LAI, crop height, and rooting depth) were specified as a function of the crop development stage. The development stage was assumed to be linear with a growth period from emergence to harvest ($0 <$ development stage < 2) (Ma et al., 2015). Extinction coefficients for diffuse and direct visible light were used as the model default values, which were 0.60 and 0.75, respectively (Hassanli et al., 2016; Jiang et al., 2016). Root growth was simplified to a static development process unrelated to climatic conditions (Kroes et al., 2017). Due to a lack of root length data, the maximum root length of winter wheat was set to 100 cm according to Jha et al. (2017). The root length of the other stages was obtained using linear interpolation of crop height (Feng, Jiang, Huo, & Zhang, 2014). Root water uptake was calculated using the macroscopic model proposed by Feddes et al. (1976). The reduction coefficient for RWU was a function of the pressure head and potential transpiration (T_p). The corresponding parameters were obtained from previous research (Cai et al., 2017; Feng et al., 2014; Yang et al., 2009) before the model was run.

2.3.2 | Top and bottom boundary conditions

The top boundary was above the crop canopy and mainly contained meteorological data such as temperature and precipitation. The bottom boundary was in the unsaturated zone. In this study, we set the bottom boundary to 100 cm below surface and it drained freely without groundwater recharge and lateral drainage.

2.3.3 | Soil water flow

The model uses the Richards equation (Richards, 1931) to describe the water movement in unsaturated soils, and RWU is the sink term $S(z)$ included in the equation (Feddes et al., 2001).

$$C(h)\frac{\partial h}{\partial t} = \frac{\partial\left[K(h)\left(\frac{\partial h}{\partial z}+1\right)\right]}{\partial z} - S(z) \quad (1)$$

where $C(h)$ is the differential water capacity (cm^{-1}), indicating the change in water content caused by the change of the unit matrix potential, and is numerically equal to the slope of the soil water characteristic; t is time (d); K is the hydraulic conductivity (cm d^{-1}); h is the soil water pressure head (cm); z is the vertical coordinate (cm) taken positively upward; and $S(z)$ is the RWU rate at a certain depth (cm^3 cm^{-3} d^{-1}).

2.3.4 | Potential transpiration, potential evaporation, and RWU rate

The SWAP model offers two methods for the distribution of T_p and evaporation (E_p). One is based on crop and soil factors and the other is a direct application of the Penman–Monteith equation. The direct application of the Penman–Monteith equation was used in this study. This method does not require crop or soil factors to translate reference ET to crop ET and avoids the complicated calibration process. T_p and E_p can be calculated following Kroes et al. (2017). The measured actual ET was calculated using the water balance method.

The macroscopic Feddes RWU models incorporate the root length density distribution, $\pi_{root}(z)$, which is considered uniform (Feddes, Kowalik, & Zaradny, 1978; Kumar, Shankar, & Jat, 2014). By considering $\pi_{root}(z)$, the potential RWU rate at a certain depth, $S_p(z)$, can be calculated by (Feddes et al., 2001; Jiang et al., 2016):

$$S_p(z) = \frac{\pi_{root}(z)}{\int_{-D_{root}}^{0}\pi_{root}(z)\partial z}T_p = \beta(z)T_p = \frac{T_p}{D_{root}} \quad (2)$$

where D_{root} is the rooting depth (cm), and $\beta(z)$ is the normalized root length density (cm^{-1}).

$S_p(z)$ is reduced due to suboptimal soil conditions: too wet, too dry, too saline or too cold. Salt stress and cold stress are not considered in this study. The water stress function $\alpha[h(z)]$ in SWAP is described by Eq. [(3)] (Feddes et al., 1978). The actual RWU $S_a(z)$ can be calculated by:

$$\alpha[h(z)] = \begin{cases} 0 & h \geq h_1, h \leq h_4 \\ \frac{h-h_1}{h_2-h_1} & h_2 \leq h < h_1 \\ 1 & h_3 < h \leq h_2 \\ \frac{h-h_4}{h_3-h_4} & h_4 < h \leq h_3 \end{cases} \quad (3)$$

$$S_a(z) = \beta(z)\alpha[h(z)]T_p \quad (4)$$

Root water uptake is zero when the soil pressure head is less than h_4 (wilting point, −16000 cm) or greater than h_1 (−1 cm) due to a lack of oxygen in the root zone. Root water uptake is unlimited when the soil pressure head is between h_2 and $h_{3,high}$ (−500 cm) for high atmospheric transpiration potential (T_{high} = 0.5 cm d^{-1}) or $h_{3,low}$ (−1000 cm) for low atmospheric transpiration potential (T_{low} = 0.1 cm d^{-1}). Root water uptake increases linearly between h_4 and h_3 and decreases linearly between h_2 and h_1 (Cai et al., 2017; Feng et al., 2014; Yang et al., 2009).

2.3.5 | Model calibration and verification

The soil physical properties of the different layers listed in Table 1 were entered into the RETC software (Van Genuchten, Leij, Yates, & Williams, 1991). Based on the artificial neural network method, the initial values (Table 4) of the Van Genuchten model were obtained (Li et al., 2018). The degree of agreement between the simulated values and the measured values was evaluated using the mean relative error (MRE) and the root mean square error (RMSE) according to the following equations (Feng et al., 2014):

$$\mathrm{MRE}(\%) = \frac{1}{N}\sum_{i=1}^{N}\left|\frac{P_i - O_i}{O_i}\right| \times 100 \quad (5)$$

$$\mathrm{RMSE} = \sqrt{\frac{1}{N}\sum_{i=1}^{N}\left(P_i - O_i\right)^2} \quad (6)$$

where P_i is the ith predicted value; O_i is the ith observed value; and N is the total number of observations.

Then, the treatments W4, W5, T4, and T5 were selected to calibrate the model. These treatments were selected because their irrigation amounts were at a medium level compared with the other treatments. This enhanced the

TABLE 4 Initial soil hydraulic parameters of the Van Genuchten model (Van Genuchten et al., 1991) obtained by the RETC software, and calibration parameters obtained by the SWAP model

Soil layer	Residual water content, θ_r		Saturated water content, θ_s		Saturated hydraulic conductivity, K_s		Water content shape factor			
							α		n	
	Initial value	Calibration value	Initial value	Calibration value	Initial value	Calibration value	Initial value	Calibration value	Initial value	Calibration value
cm	$cm^3\ cm^{-3}$				$cm\ d^{-1}$					
0–20	0.07	0.10	0.43	0.42	19.37	15.00	0.01	0.040	1.61	1.30
20–40	0.07	0.13	0.41	0.41	13.12	15.00	0.01	0.030	1.61	1.70
40–60	0.07	0.10	0.41	0.49	13.56	10.00	0.01	0.035	1.62	1.70
60–80	0.07	0.10	0.41	0.47	13.56	10.00	0.01	0.040	1.62	1.70
80–100	0.07	0.10	0.41	0.45	13.56	7.00	0.01	0.045	1.62	1.55

representativeness of the calibration results. According to the range of soil hydraulic characteristics measured or simulated (Gao & Shao, 2011; Yao & Shao, 2015), we adjusted the corresponding parameters in SWAP until MRE ≤20% and RMSE ≤0.05 $cm^3\ cm^{-3}$. The adjusted parameters were used for model verification in all other treatments.

2.4 | Path analysis

Before establishing the simplified RWU model, stepwise regression analysis was utilized to screen the independent variables initially. However, the simple correlation coefficient did not provide a comprehensive link between the tested indicators and the RWU (Hladni, Jocic, Mijic, Miklic, & Miladinovic, 2016). Therefore, the correlation coefficient was further analyzed using a path analysis (Wright, 1921) that included the direct and indirect effects (Astereki, Sharifi, & Pouresmael, 2017). The first variable from the meteorological, crop and soil indicators was selected based on the order of the decision coefficient (DC). Under the premise of ensuring representativeness, fewer variables were utilized to extend the scope of the simplified RWU model using multiple nonlinear regression. SPSS 21 (IBM, Armonk, NY, USA) was used for the regression and path analyses.

2.5 | Statistical analysis

We analyzed the RWU of each soil layer under different irrigation scenarios using analysis of variance (ANOVA) with SPSS. The ANOVA was performed at the $\alpha = 0.01$ level of significance to determine if significant differences existed among the treatment groups. Mean comparisons were performed for significant effects with the least significant difference (LSD) test at $\alpha = 0.01$. The differences between the treatments were considered significant at $P < 0.01$.

3 | RESULTS

3.1 | Evaluation of model performance

The SWC simulated by the SWAP model was in good agreement with the measured values (Figure 1). The MRE was 4.7 to 21.7% (Table 5) and the RMSE was 0.01 to 0.07 $cm^3\ cm^{-3}$, both of which were within the acceptable range. Statistical analysis showed that the simulated SWC and ET (Table 6) were in good agreement ($R^2 = 0.417$; $P < 0.01$) and correlated with the measured values. These results indicated that SWAP model can be used to predict the field water status.

3.2 | Profile distribution of RWU

Table 7 showed cumulative RWU in different layers of the 100 cm root zone. The cumulative RWU of the surface layer (0–20 cm) was the largest (117.86–152.23 mm) with 49.6% of total root zone. Then, the cumulative RWU gradually decreased with the soil layer. The cumulative RWU portion of the 0- to 60-cm soil layer was 89.4%. This indicated that the main source of RWU was located in the 0- to 60-cm soil layer. The results of ANOVA showed that there was a significant ($P < 0.01$) difference in cumulative RWU of 0 to 60 cm, while 60 to 100 cm was not different. This meant that the RWU was sensitive to SWC, but that sensitivity varied among different soil layers. For treatments T3 and T8 (Figure 2), the root of the 40- to 60-cm soil layer stopped absorbing water due to serious water deficit during grain filling to maturity, but the root of the other layers did not stop absorbing water.

3.3 | Effects of water stress on RWU at different growth stages

The cumulative RWU at different growth stages are listed in Table 7. The cumulative RWU reached a maximum during

TABLE 5 Mean relative error (MRE) and root mean square error (RMSE) and calibration and verification results for soil water content simulated by the SWAP model in the 2012 to 2013 and 2013 to 2014 growing seasons

		Soil layer									
		0–20 cm		20–40 cm		40–60 cm		60–80 cm		80–100 cm	
		MRE	RMSE	MRE	RMSE	MRE	RMSE	MRE	RMSE	MRE	RMSE
Year	Treatment	%	$cm^3\ cm^{-3}$	%	$cm^3\ cm^{-3}$	%	$cm^3\ cm^{-3}$	%	$cm^3\ cm^{-3}$	%	$cm^3\ cm^{-3}$
2012–2013	W1	17.59	0.04	11.12	0.03	19.11	0.05	15.39	0.04	19.19	0.05
	W2	14.57	0.03	11.96	0.03	7.91	0.02	7.29	0.02	14.81	0.04
	W3	14.94	0.03	16.49	0.04	13.78	0.04	6.78	0.02	14.56	0.04
	W4[a]	17.36	0.04	18.52	0.04	7.44	0.02	7.08	0.02	15.78	0.04
	W5[a]	13.41	0.03	12.14	0.03	10.76	0.03	6.84	0.02	12.19	0.03
	W6	13.30	0.03	14.16	0.03	10.00	0.03	6.38	0.02	10.81	0.03
	W7	11.77	0.03	11.39	0.03	7.36	0.02	6.08	0.02	13.46	0.03
	W8	12.77	0.03	12.01	0.03	9.40	0.03	5.00	0.02	9.99	0.03
	W9	12.26	0.03	15.53	0.04	8.62	0.02	12.55	0.04	4.75	0.01
2013–2014	T1	6.92	0.02	16.10	0.04	9.22	0.03	14.82	0.05	11.83	0.04
	T2	11.82	0.03	17.92	0.05	17.00	0.05	20.71	0.07	11.08	0.04
	T3	9.73	0.03	21.97	0.06	19.22	0.05	14.59	0.04	4.71	0.02
	T4[a]	8.92	0.03	19.51	0.05	16.36	0.05	18.13	0.05	12.09	0.04
	T5[a]	16.26	0.04	14.81	0.04	13.35	0.04	11.39	0.04	9.08	0.03
	T6	11.03	0.03	21.53	0.05	16.97	0.05	18.92	0.06	5.45	0.02
	T7	12.86	0.04	18.26	0.05	11.51	0.03	21.66	0.06	12.00	0.04
	T8	9.11	0.03	21.77	0.05	17.68	0.05	20.16	0.06	8.11	0.03
	T9	15.07	0.04	18.54	0.05	13.87	0.04	11.20	0.03	10.32	0.03

[a]Treatments used for model calibration. All other treatments were used for model verification.

TABLE 6 Field water balance and yield under different irrigation treatments during the 2012 to 2013 and 2013 to 2014 growing seasons. Water budget included deep leakage (D), soil storage water consumption (ΔW, a positive value indicates a decrease in soil water storage), and evapotranspiration (ET) by the water balance method

		Simulated value			Measured value	
		D	ΔW	ET	ET	Yield
Year	Treatment	mm				$kg\ hm^{-2}$
2012–2013	W1	19.42	72.05	389.63	410.09	7067.76
	W2	33.54	108.84	361.31	362.55	6443.62
	W3	18.24	112.88	329.64	328.25	6299.75
	W4	5.86	84.72	346.86	355.63	5538.26
	W5	11.90	90.08	349.18	349.94	6874.58
	W6	11.60	91.36	353.76	346.42	7316.76
	W7	7.95	95.17	340.23	345.92	5695.27
	W8	5.58	77.47	327.89	321.54	6512.22
	W9	1.51	49.02	306.51	291.55	4384.44
2013–2014	T1	36.86	91.03	318.17	322.52	6717.24
	T2	23.44	96.36	300.92	289.37	6241.05
	T3	19.15	95.46	268.31	258.89	4234.95
	T4	15.07	95.07	285.00	282.22	5683.25
	T5	26.65	109.13	314.49	301.70	5841.84
	T6	7.60	68.65	257.05	253.63	5882.07
	T7	6.01	82.38	287.37	275.74	5886.02
	T8	4.05	86.58	257.53	245.21	5692.49
	T9	7.37	89.66	284.29	284.00	5008.08

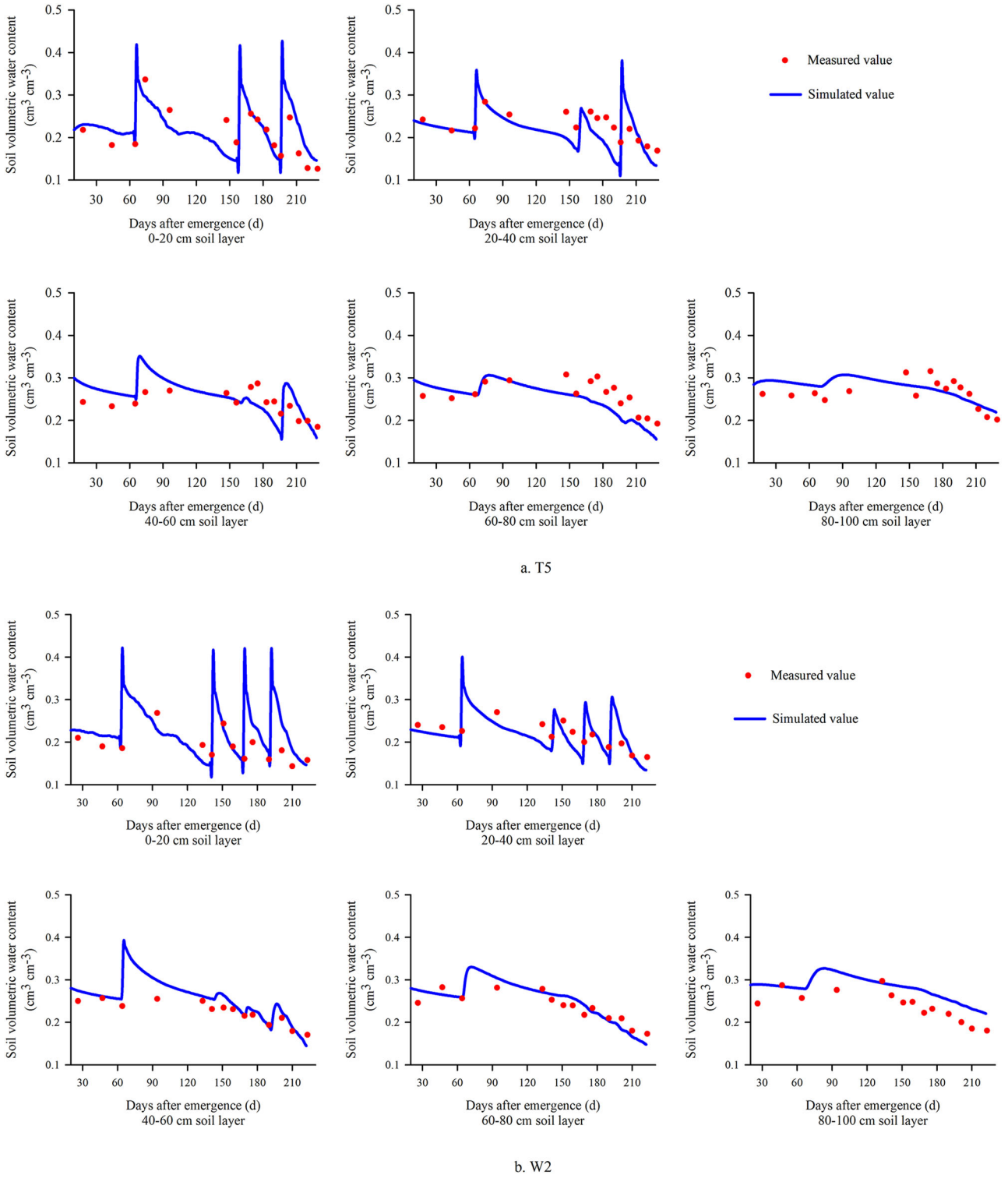

FIGURE 1 Simulated and measured values of soil water content of (a) treatment T5 used for calibration, and (b) treatment W2 used for verification

the late growth stage of the two growing seasons (grain filling to maturity in 2012–2013 and heading to maturity in 2013–2014). The portion from jointing to heading was the smallest, accounting for 21% (2012–2013 growing season) and 17% (2013–2014 growing season) of the total growth stage. The regression analysis showed that yield was in good agreement ($R^2 = 0.376$; $P < 0.01$) with cumulative RWU during the total growth period.

We selected 1 d (78, 162, 178, and 205 d after emergence) from each of the four growth stages to compare RWU of

TABLE 7 Cumulative root water uptake at different soil layers (0–20, 20–40, 40–60, 60–80, and 80–100 cm) and different growth stages (emergence to jointing, jointing to heading, heading to grain filling and grain filling to maturity) for winter wheat in the 2012 to 2013 and 2013 to 2014 growing seasons

		Soil layer					Growth stage			
		0–20 cm	20–40 cm	40–60 cm	60–80 cm	80–100 cm	Emergence to jointing	Jointing to heading	Heading to grain filling	Grain filling to maturity
Year	Treatment	mm								
2012–2013	W1	148.44	78.78	44.31	23.75	6.81	63.85	58.46	65.41	114.36
	W2	152.23	82.66	47.05	23.72	6.92	72.92	65.28	69.84	104.54
	W3	140.14	70.30	26.28	21.98	6.77	75.96	57.77	59.60	72.15
	W4	151.32	83.92	39.95	22.73	6.91	72.66	71.38	73.36	87.42
	W5	140.72	80.79	44.95	23.35	6.41	67.21	62.39	60.53	106.10
	W6	148.38	80.53	47.62	24.20	6.38	70.32	59.52	69.26	108.01
	W7	137.79	76.78	43.61	22.00	5.96	60.22	59.50	65.27	101.15
	W8	130.45	73.58	45.11	23.67	6.40	51.93	58.22	64.76	104.29
	W9	122.09	72.89	44.23	20.81	5.88	45.35	54.16	61.41	104.98
2013–2014	T1	144.11	69.84	46.05	24.26	6.05	71.44	45.68	86.55	86.64
	T2	141.12	65.07	43.60	22.80	6.98	79.66	45.86	79.90	74.16
	T3	135.07	52.74	27.66	22.26	6.97	81.67	46.04	64.25	52.75
	T4	137.40	61.90	34.76	23.16	6.22	75.54	45.00	84.24	58.67
	T5	143.63	67.20	47.92	25.76	6.68	77.01	45.81	79.56	88.81
	T6	117.86	55.76	38.84	21.14	6.63	58.11	46.20	65.63	70.29
	T7	130.58	65.81	44.29	21.65	6.60	65.18	44.65	84.54	74.56
	T8	127.94	55.65	27.52	19.72	7.19	70.59	43.98	73.67	49.78
	T9	125.30	58.70	44.66	24.26	6.67	65.21	45.10	64.58	84.70

different irrigation treatments (Figure 3). The effect of water stress on RWU from heading to grain filling was observed from treatments W4 and W7 (Figure 3a). The irrigation was 75 mm (W4 and W7) during jointing to heading, and was 72 mm (W4) and 54 mm (W7) during heading to grain filling. The RWU rate of W4 was faster than W7 in each soil layer at 178 d (heading to grain filling). However, the opposite effect of the water stress was observed in the emergence to jointing stage. For instance, irrigation of T1 was 32 mm higher than T8, but the RWU rate was slightly lower than T8 at 78 d (Figure 3c).

We analyzed the maximum RWU rate under different irrigation levels to reflect the sensitivity of the growth stage to water stress. The results revealed that water stress caused different degrees of inhibition for RWU, except for emergence to jointing (Figure 3c). Water stress had the strongest effect on RWU during heading to grain filling, and the difference of the maximum RWU rate was 0.0020 to 0.0026 $cm^3\ cm^{-3}\ d^{-1}$. For the jointing to heading and grain filling to maturity, the difference was 0.0006 to 0.0012 $cm^3\ cm^{-3}\ d^{-1}$. This indicated that the RWU sensitivity of these two growth stages was relatively low. As shown in Figure 3b, the RWU rate at 205 d had small differences.

The SWC when the RWU was 95% of the control treatment was set as the critical SWC. As described in Table 8, the critical SWC (from all treatments other than the control) of different growth stages was as follows: emergence to jointing > jointing to heading > grain filling to maturity > heading to grain filling. They were equivalent to 92.1, 68.6, 67.7, and 66.9% of the field capacity, respectively. The critical SWC decreased with the depth of the soil layer, reaching the minimum at 60 to 80 cm (0.19 $cm^3\ cm^{-3}$), and then increased to 0.24 $cm^3\ cm^{-3}$ at the 80- to 100-cm layer.

3.4 | Resumption of RWU after rewetting

Resumption of RWU after rewetting is essential for plant growth (Nulsen & Thurtell, 1978). The maximum RWU rate after rewetting of the control treatments (W1 and T1) was used as a reference. The maximum values of other treatments were divided by the reference to evaluate the recovery degree of RWU. For the 2012–2013 growing season, RWU recovered after rewetting during emergence to heading, but did not match the control level during heading to maturity. The recovery degree of RWU during heading to grain filling was the lowest (average 93.7%), followed by grain filling to maturity (average 97.5%). RWU practically recovered in all growth stages in 2013–2014. The recovery degree of first three growth periods was 108.3%, 101.4 and 102.8%,

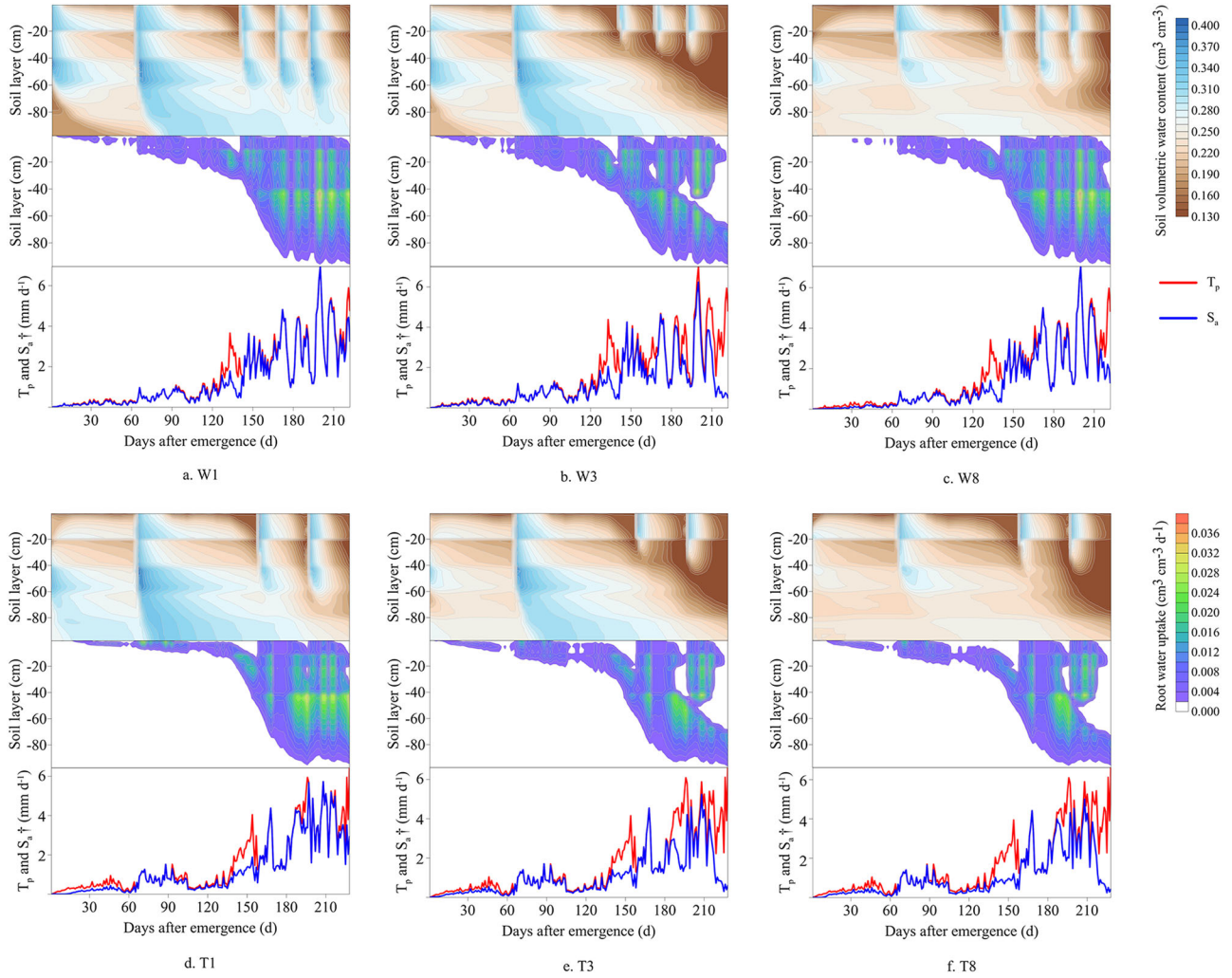

FIGURE 2 Soil water content and root water uptake contour map of winter wheat for (a-c) treatments W1, W3, and W8 of the 2012 to 2013 growing season, and (d-f) treatments T1, T3, and T8 of the 2013 to 2014 growing season. † Potential plant transpiration (T_p) and actual root water uptake (S_a)

TABLE 8 Critical soil water content when the root water uptake rate is 95% of the control treatment at different soil layers (0–20, 20–40, 40–60, 60–80, and 80–100 cm) and different growth stage (emergence to jointing, jointing to heading, heading to grain filling and grain filling to maturity) for winter wheat in the 2012 to 2013 and 2013 to 2014 growing seasons

Soil layer	Emergence to jointing	Jointing to heading	Heading to grain filling	Grain filling to maturity
cm	cm^3 cm^{-3}			
0–20	0.31	0.25	0.26	0.27
20–40		0.21	0.22	0.24
40–60		0.24	0.20	0.22
60–80			0.20	0.19
80–100			0.25	0.24

respectively. This may be due to the fact that irrigation during heading to grain filling in 2013–2014 was more than in 2012–2013. In summary, the order of RWU resumption ability was as follows: emergence to jointing > jointing to heading > grain filling to maturity > heading to grain filling. This order was consistent with the results of the critical SWC mentioned above. Therefore, we can obtain information about RWU recovery based on the critical SWC, which is more convenient to measure.

The above phenomenon was observed intuitively from the RWU rate contour map (Figure 2). This figure also reflects the impacts on RWU due to SWC, $\beta(z)$ and $\alpha[h(z)]$

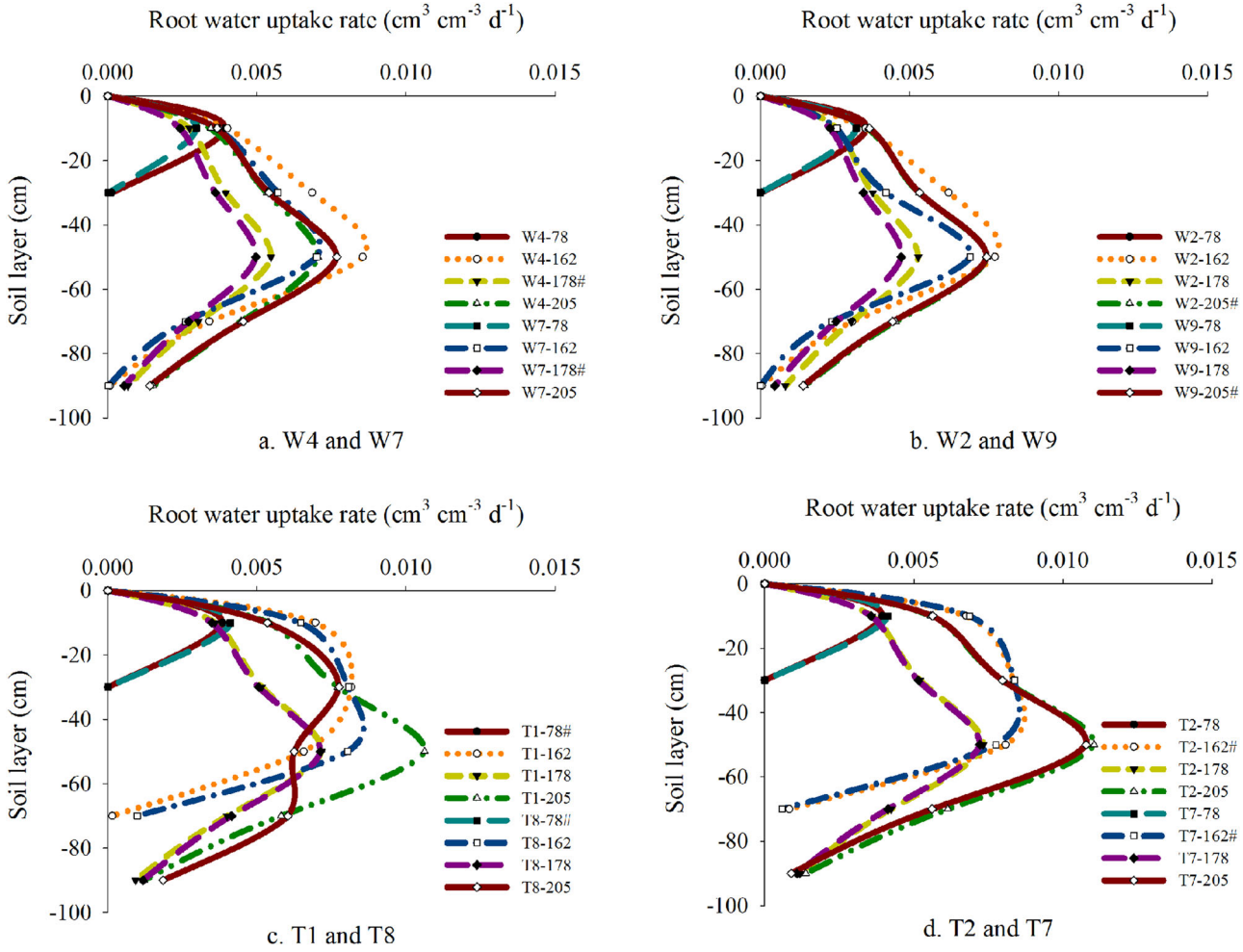

FIGURE 3 Profile distribution (0–100 cm) of the root water uptake rate for winter wheat at different growth stages (78, 162, 178, and 205 d after emergence) under (a-b) treatments W4, W7, W2 and W9 of the 2012 to 2013 growing season, and (c-d) treatments T1, T8, T2, and T7 of the 2013 to 2014 growing season. In figure legend, the number sign (#) indicates key contrast treatments

functions, and potential plant transpiration (T_p). When SWC reduced to a certain extent, RWU decreased due to water stress. Then, $\beta(z)\alpha[h(z)]$ decreased and RWU also decreased accordingly. The change of actual RWU (S_a) was consistent with T_p. Because the time interval between the first irrigation and emergence was long, the root stopped absorbing water (white area in 20-cm soil layer) at approximately 150 d. The stagnation of RWU lasted for ~15 d. Root water cessation also occurred during heading to grain filling (Figure 2b, e, f), but the duration (mainly observed in the 40-cm soil layer) was shorter, approximately 3 to 7 d. Although RWU decreased, it recovered after rewetting in these two stages. Treatments W3, T3 and T8 were treated as severe water deficit during grain filling to maturity. Then the duration of stagnation increased, and the affected depth also expanded to 20 to 80 cm.

The recovery time required for maximum RWU is another important indicator of the response to water stress. We found that RWU did not recover immediately after rewetting, namely, there was a hysteresis effect. In the 2012–2013 growing season, the recovery time of the four growth stages were 2 d, 5 d, 5 d, and 8 d after irrigation, respectively. During the 2013–2014 growing season, the recovery time in each stage increased (6 d, 9 d and 11 d).

3.5 | Path and regression analysis for RWU

Stepwise linear regression analysis with RWU as the dependent variable y eliminated the following independent variables x: average SWC of 0 to 20 cm (x_3–SWC20), average SWC of 0 to 40 cm (x_4–SWC40) and average temperature (x_8–temperature). The $R^2 = 0.821$ of linear regression was acceptable, but the model established had too many independent variables. Then, RWU was used as a dependent variable, and the residual factors served as the independent variables for path analysis. The direct and indirect effects were listed

in Table 9. Among the variables, crop height, radiation, average SWC of 0 to 60 cm (SWC60) and average SWC of 0 to 80 cm (SWC80) had strong direct effect (absolute value 0.329–0.599) on RWU, and the other variables had very little effect. The direct effect of crop height, radiation, and SWC60 were positive, and the SWC80 was negative (−0.416). The direct effects of other variables were negligible (absolute values were less than 0.100). Based on the sum of indirect effects, LAI and SWC60 had the largest positive (0.644) and negative (−0.755) effect, respectively. The simple correlation coefficient between each variable and RWU was the sum of the direct effect and total indirect effect. The simple correlation coefficient reflects the positive and negative correlation between the variable and RWU (de Almeida Rios et al., 2018; Seker & Serin, 2004). The crop height, radiation, and LAI had extremely significant ($P < 0.01$) correlations with RWU. Except for RH, SWC60, SWC80 and SWC of the 0- to 100-cm soil layer (SWC100), simple correlation coefficients of the other variables were positive. This indicated that excessive RH and SWC significantly ($P < 0.01$) inhibited RWU. The simple correlation coefficient of SWC60 was weaker in comparison to the direct effect, namely, the relation had been masked by the negative indirect effect through SWC80 (−0.406) and crop height (−0.233). The simple correlation coefficient of LAI was significantly ($P < 0.01$) positive in comparison to the direct effect, namely, the relation had been enhanced by the positive indirect effect through crop height (0.493) and SWC80 (0.190). Crop height and radiation had significantly ($P < 0.01$) positive correlation coefficients and strong direct effects. This indicated that the two variables promoted RWU jointly (Seker & Serin, 2004). Among the meteorological factors, the DC was as follows: x_{10}–radiation (0.357) > x_{11}–wind speed (0.020) > x_9–RH (0.011). Among the crop factors, the DC was: x_2–crop height (0.651) > x_1–LAI (0.096). Among the soil factors, the DC was as follows: x_5–SWC60 (−0.508) > x_6–SWC80 (0.119) > x_7–SWC100 (−0.012).

We selected the first variable (x_2–crop height, x_{10}–radiation, and x_5–SWC60) based on DC to build the next simplified RWU model. Crop height was an important factor connecting meteorological with SWC and played a key role in RWU. Radiation affects RWU through plant transpiration. The DC for SWC of the 0- to 60-cm layer was the largest. This emphasized the importance of the 0- to 60-cm soil layer to RWU. By observing the RWU of the 0- to 100-cm root zone (Figure 2), we found that the curve was closer to the exponential function. Therefore, we established an exponential function to estimate RWU by nonlinear regression analysis ($R^2 = 0.856$; $P < 0.01$):

$$S = \exp[0.031(\mathrm{CH}) + 0.065(\mathrm{RAD}) + 2.649(\mathrm{SWC60}) - 6.843] \quad (7)$$

TABLE 9 Direct and indirect effects of predictor variables on root water uptake for winter wheat

Independent variable[a]	Simple correlation coefficient with y[b]	Direct effect	Indirect effect							Total indirect effect	DC[c]
			x_2, Crop height	x_{10}, Radiation	x_{11}, Wind speed	x_1, LAI	x_9, RH	x_6, SWC80	x_5, SWC60	x_7, SWC100	
x_2, Crop height	0.843**	0.599		0.185	0.009	0.058	−0.002	0.201	−0.197	−0.009	0.245	0.651
x_{10}, Radiation	0.707**	0.329	0.336		0.005	0.030	0.015	0.144	−0.148	−0.005	0.377	0.357
x_{11}, Wind speed	0.180**	0.071	0.077	0.023		0.006	0.012	0.030	−0.031	−0.006	0.109	0.020
x_1, LAI	0.715**	0.071	0.493	0.142	0.006		−0.004	0.190	−0.190	0.008	0.644	0.096
x_9, RH	−0.134**	−0.050	0.028	−0.099	−0.017	0.005		0.058	−0.065	0.005	−0.084	0.011
x_6, SWC80	−0.351**	−0.416	−0.289	−0.114	−0.005	−0.032	0.007		0.492	0.007	0.066	0.119
x_5, SWC60	−0.252**	0.504	−0.233	−0.097	−0.004	−0.027	0.006	−0.406		0.006	−0.755	−0.508
x_7, SWC100	−0.119**	0.044	−0.127	−0.037	−0.010	0.014	−0.006	−0.064	0.068		−0.162	−0.012

** difference at the 0.01 probability level.

[a]Independent variables x included crop height (cm), radiation (MJ m^{-2}), wind speed at 2-m height (m s^{-1}), leaf area index (LAI, m^2 m^{-2}), relative humidity (RH, %), and average soil water content (SWC, cm^3 cm^{-3}) at 0 to 60, 0 to 80, and 0 to 100 cm.

[b]Dependent variable y was root water uptake.

[c]DC, decision coefficient of independent variable.

where S is RWU of 0- to 100-cm root zone (cm d^{-1}); CH is the crop height (cm); RAD is the radiation (MJ m^{-2}); and SWC60 is an average SWC of the 0- to 60-cm soil layer (cm^3 cm^{-3}).

To enhance the applicability of the simplified RWU model and reflect the dynamic change of RWU, we constructed a function of RWU over time. By regression analysis on crop height and days after emergence, we found that both cubic functions ($R^2 = 0.918$) and power functions ($R^2 = 0.911$) reflected their relationship well ($P < 0.01$). For the purpose of minimizing the number of parameters, we chose the power function on days after emergence (DAE) to construct an improved simplified RWU model ($R^2 = 0.836$; $P < 0.01$):

$$S = \exp\left[-52.165(\mathrm{DAE}^{-0.447}) + 0.062(\mathrm{RAD}) + 4.035(\mathrm{SWC60})\right] \quad (8)$$

Figure 4 compares the RWU simulated by the SWAP model and the values calculated using the simplified RWU model (W5 and T5). The R^2 was 0.720 to 0.912 ($P < 0.01$) for other treatments. This meant that the reliability of the simplified RWU model was strong. Under conditions with few parameters, it was suitable to estimate RWU for winter wheat.

4 | DISCUSSION

4.1 | Profile of RWU for winter wheat

Irrigation had a significant ($P < 0.01$) impact on RWU in the upper soil layer. Similar results were found by previous researchers (Li, Zhou, Sun, Wang, & Gao, 2014; Xue et al., 2003). Irrigation changes the soil water distribution and oxygen status, which was the main reason for the impact on physiological activities of the roots. After irrigation at the emergence to jointing stage, the root system extended to the 20- to 40-cm soil layer. We found that severe water deficit treatment at this stage promoted cumulative RWU. Cai et al. (2017) observed the same effect. This may be due to the compensation effect of root growth stimulated by drought. High irrigation may maintain a higher SWC in the upper soil layer, which meet the needs of the plant, while water stress promotes root elongation to deeper soils. The profile distribution of RWU was affected by root development, distribution (Green & Clothier, 1995) and SWC. The reason why cumulative RWU was concentrated in the upper soil layer was that most winter wheat roots were located in the upper 40 cm (Zhang et al., 2004). Root water uptake decreased with depth due to the gradual decrease in the availability of soil water. As the SWC of top soil decreased, the RWU gradually moved to the deep layer. The same phenomenon was observed previously (Jha et al., 2017).

Root growth is a process in which the assimilation products are assigned to the appropriate location of the plant, and this is adjusted at the entire plant level (Engels, Mollenkopf, & Marschner, 1994). Therefore, it is necessary to use the compensation effect of roots and the distribution pattern of RWU in actual agricultural production. This helps the root enhance the utilization of deep soil water and nutrients for achieving the goal of water saving irrigation.

4.2 | Pattern of RWU under water stress at different growth stages

The roots of winter wheat gradually develop during the growth period until senescence and loss of activity (Cai et al., 2018). During heading to maturity, the RWU rate and accumulated value reached the maximum. This indicated that winter wheat needs more water during the reproductive growth than during the vegetative stage. Because this is the rapid growth stage of winter wheat, the root grows vigorously and the transpiration intensity is the highest (Guo et al., 2018). Therefore, one must ensure that there is enough of a water supply at heading to maturity. Understanding the sensitivity of RWU at different growth stages helps with more precise irrigation management. Our findings clarified that water stress at heading to grain filling reduced RWU in all layers (Figure 3a). RWU may also be influenced by the hydraulic conductivity of the root at this stage (Nobel & Huang, 1992). The absorbing capacity was reduced because the root growth stagnated and suberization increased, both of which decreased the water permeability of the root surface (Kramer, 1950). We found that RWU was less sensitive to SWC during grain filling to maturity than other stages. This may be because winter wheat had established a complete root system, and the tolerance to water stress had increased. This is consistent with the results of Xue et al. (2003), who found that winter wheat had a similar root density at this stage for different treatments. According to the change of critical SWC in different soil layers, we suggest that SWC of a winter wheat field should not be lower than 60% of field capacity (Yu et al., 2016; Yu, Cai, Zheng, Li, & Wang, 2017). Otherwise, the water stress will have adverse effects on RWU and hinder the healthy growth of crops.

4.3 | Resumption of RWU after rewetting

Moderate water stress did not stop the roots from absorbing water, and the RWU recovered after rewetting. This observation was agreement with the findings of other researchers (Ahmed et al., 2016; Benard, Kroener, Vontobel, Kaestner, & Carminati, 2016). Even if the water deficit was severe and some plants withered, most plants recovered within a few hours or days (Kramer, 1950). Previous research

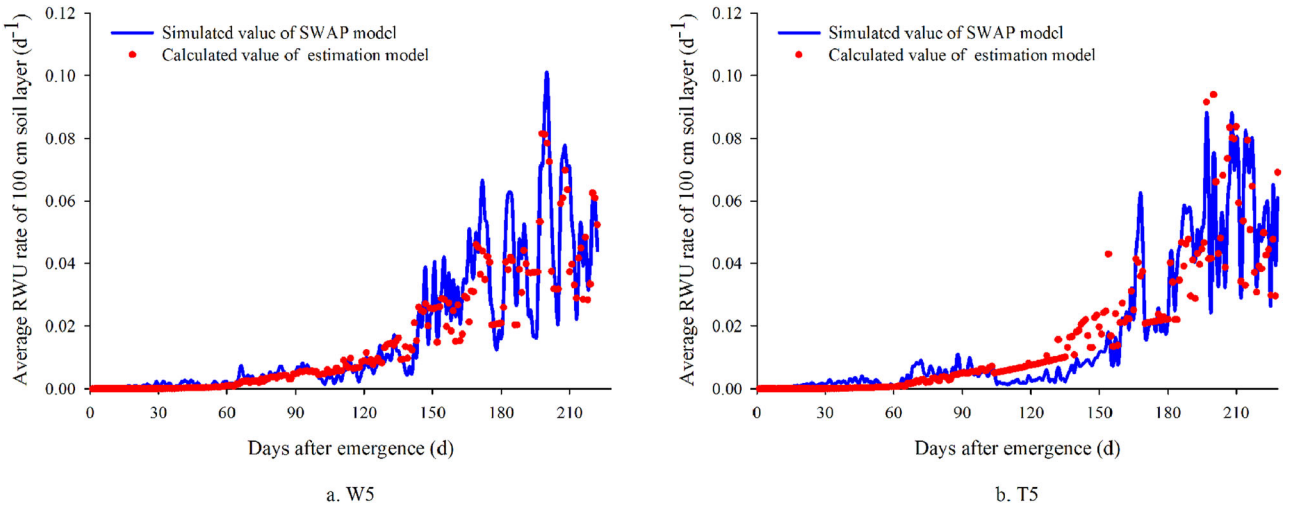

FIGURE 4 Root water uptake (RWU) simulated by the SWAP model and the values calculated by the simplified RWU model in the 0- to 100-cm soil layer in (a) treatment W5 of the 2012 to 2013 growing season, and (b) treatments T5 of the 2013 to 2014 growing season

(Carminati et al., 2010) showed that the rhizosphere prevented water loss from the roots when subjected to water stress. Ahmed et al. (2016) and Benard et al. (2016) found that this dynamic behavior of the rhizosphere was the effect of mucilage. The mucilage is a gelatinous material secreted by the root tips and is capable of absorbing large amounts of water under dry conditions (McCully & Boyer, 1997). The compensating effect of RWU was also observed after rewetting, especially in the emergence to heading stage. This suggested that the RWU recovered after water stress, and even exceeded the treatments with more irrigation. This may be due to the inactive roots caused by drought quickly recovered activity after rewetting. Green and Clothier (1995) found that root activities after rewetting were greater than during the drying period. Cai et al. (2018) concluded that new root growth was a mechanism leading to RWU activity increase after rewetting.

In addition to the compensation effect, we also observed a hysteresis effect in the RWU recovery period. After rewetting, RWU usually took several days to reach the maximum value. Similar results were also obtained by previous researchers (Carminati et al., 2010; Zarebanadkouki et al., 2018; Zarebanadkouki, Ahmed, & Carminati, 2016). They found that the rhizosphere was wetter than the soil during drying, but stayed temporarily dry after rewetting. It indicated that the hydraulic properties of the rhizosphere were hysteretic and time-dependent. The mucilage contained a small fraction of amphiphilic components such as lipids (Moradi et al., 2012). The component caused hydrophobicity in the rhizosphere during drying. Hydrophobicity temporarily limited the water throughout the rhizosphere interface (Zarebanadkouki et al., 2016). However, this was not always negative because it prevented severe root dehydration and kept root vitality during drought (Zarebanadkouki et al., 2018).

The duration of water stress affected the RWU recovery. Treatments W3 and W8 were subjected to the most severe water stress at grain filling to maturity, but RWU of W3 did not recover during grain filling to maturity (Figure 2). Root water uptake of W3 was only 46.5% of the control in the 40- to 60-cm soil layer. This was because W8 was fully irrigated during the previous growth stage, whereas W3 remained in a severe deficit. This indicated that transient water stress promoted RWU recovery and long-term stress caused adverse effects (Kramer, 1950; Wraith, Baker, & Blake, 1995). In summary, from the perspective of recovery ability and time required for RWU, for winter wheat severe water deficit during grain filling to maturity should be avoided as much as possible.

5 | CONCLUSIONS

The calibrated SWAP model performs well in simulating SWC and farmland water balance. The model can be used as an effective method to quantitatively study water conversion in the field. The reliability of the simplified RWU model was strong, and it was suitable to estimate the RWU for winter using few parameters. RWU is an important component of farmland water balance, which determines the actual plant transpiration. It is closely related to root growth, SWC and meteorological conditions. Therefore, it is necessary to formulate a reasonable irrigation schedule to optimize RWU. Based on the profile distribution, the RWU in the 0- to 60-cm soil layer accounts for nearly 90% of the total root zone. Irrigation has a significant effect on RWU in this area, but not in the deeper layers. Therefore, we conclude that the SWC of the 0- to 60-cm soil layer should be maintained through reasonable irrigation methods. This will ensure that winter

wheat uses soil water more efficiently. Based on the growth stage, RWU is maximum at heading to the maturity stage. Water stress during this stage reduces the RWU recovery ability and increase recovery time. We conclude that during the implementation of deficit irrigation, water stress should be applied at early stages of growth. Sufficient water supply should be provided at later stages. This type of irrigation can make the winter wheat acquire drought tolerance at early stage, and increase RWU through a compensation effect. This also simultaneously prevents the irreversible damage caused by water stress at the heading to maturity stage. Thus, it is recommended that the SWC be kept above 60% field capacity during any growth stage. This will prevent serious RWU reduction and ensure the growth of winter wheat.

ACKNOWLEDGMENTS

This research was supported by the National Key Research and Development Program of China [grant no. 2016YFC0400200]; and National Natural Science Foundation of China [grant no. 51879223]. We thank Zhi-Jun Li and Jian Wang for their valuable assistance in the experimental work.

ORCID

Huanjie Cai https://orcid.org/0000-0002-6859-2669

REFERENCES

Ahmed, M. A., Kroener, E., Benard, P., Zarebanadkouki, M., Kaestner, A., & Carminati, A. (2016). Drying of mucilage causes water repellency in the rhizosphere of maize: Measurements and modelling. *Plant Soil*, *407*, 161–171. https://doi.org/10.1007/s11104-015-2749-1

Andarzian, B., Bannayan, M., Steduto, P., Mazraeh, H., Barati, M. E., Barati, M. A., & Rahnama, A. (2011). Validation and testing of the AquaCrop model under full and deficit irrigated wheat production in Iran. *Agricultural Water Management*, *100*, 1–8. https://doi.org/10.1016/j.agwat.2011.08.023

Astereki, H., Sharifi, P., & Pouresmael, M. (2017). Correlation and path analysis for grain yield and yield components in chickpea (Cicer arietinum L.). *Genetika*, *49*, 273–284. https://doi.org/10.2298/GENSR1701273A

Babazadeh, H., Sarai Tabrizi, M., & Homaee, M. (2017). Basil root water uptake derived models under combined water and nitrogen deficit conditions. *Irrigation and Drainage*, *66*, 377–386. https://doi.org/10.1002/ird.2104

Benabdelouahab, T., Balaghi, R., Hadria, R., Lionboui, H., Djaby, B., & Tychon, B. (2016). Testing Aquacrop to simulate durum wheat yield and schedule irrigation in a semi-arid irrigated perimeter in Morocco. *Irrigation and Drainage*, *65*, 631–643. https://doi.org/10.1002/ird.1977

Benard, P., Kroener, E., Vontobel, P., Kaestner, A., & Carminati, A. (2016). Water percolation through the root-soil interface. *Advances in Water Resources*, *95*, 190–198. https://doi.org/10.1016/j.advwatres.2015.09.014

Bonfante, A., Basile, A., Acutis, M., De Mascellis, R., Manna, P., Perego, A., & Terribile, F. (2010). SWAP, CropSyst and MACRO comparison in two contrasting soils cropped with maize in Northern Italy. *Agricultural Water Management*, *97*, 1051–1062. https://doi.org/10.1016/j.agwat.2010.02.010

Cai, G., Vanderborght, J., Couvreur, V., Mboh, C. M., & Vereecken, H. (2017). Parameterization of root water uptake models considering dynamic root distributions and water uptake compensation. *Vadose Zone Journal*, *17*, 160125. https://doi.org/10.2136/vzj2016.12.0125

Cai, G., Vanderborght, J., Langensiepen, M., Schnepf, A., Hüging, H., & Vereecken, H. (2018). Root growth, water uptake, and sap flow of winter wheat in response to different soil water conditions. *Hydrology and Earth System Sciences*, *22*, 2449–2470. https://doi.org/10.5194/hess-22-2449-2018

Cao, X., Yang, P., Engel, B. A., & Li, P. (2018). The effects of rainfall and irrigation on cherry root water uptake under drip irrigation. *Agricultural Water Management*, *197*, 9–18. https://doi.org/10.1016/j.agwat.2017.10.021

Carminati, A., Moradi, A. B., Vetterlein, D., Vontobel, P., Lehmann, E., Weller, U., … Oswald, S. E. (2010). Dynamics of soil water content in the rhizosphere. *Plant Soil*, *332*, 163–176. https://doi.org/10.1007/s11104-010-0283-8

de Almeida Rios, S., Vieira, R. N., da Cunha, Lopes, R., Barcelos, E., Nonato Carvalho da Rocha, R., & Alves de Lima, W. A. (2018). Correlation and path analysis for yield components in dura oil palm germplasm. *Industrial Crops and Products*, *112*, 724–733. https://doi.org/10.1016/j.indcrop.2017.12.054

de Jong van Lier, Q., Wendroth, O., & van Dam, J. C. (2015). Prediction of winter wheat yield with the SWAP model using pedotransfer functions: An evaluation of sensitivity, parameterization and prediction accuracy. *Agricultural Water Management*, *154*, 29–42. https://doi.org/10.1016/j.agwat.2015.02.011

Doussan, C., Pierret, A., Garrigues, E., & Pagès, L. (2006). Water uptake by plant roots: II– Modelling of water transfer in the soil root-system with explicit account of flow within the root system– comparison with experiments. *Plant Soil*, *283*, 99–117. https://doi.org/10.1007/s11104-004-7904-z

Eitzinger, J., Trnka, M., Hosch, J., Zalud, Z., & Dubrovsky, M. (2004). Comparison of CERES, WOFOST and SWAP models in simulating soil water content during growing season under different soil conditions. *Ecological Modelling*, *171*, 223–246. https://doi.org/10.1016/j.ecolmodel.2003.08.012

Engels, C., Mollenkopf, M., & Marschner, H. (1994). Effect of drying and rewetting the topsoil on root growth of maize and rape in different soil depths. *Zeitschrift für Pflanzenernährung und Bodenkunde*, *157*, 139–144. https://doi.org/10.1002/jpln.19941570213

Feddes, R. A., Hoff, H., Bruen, M., Dawson, T., de Rosnay, P., Dirmeyer, P., … Pitman, A. J. (2001). Modeling root water uptake in hydrological and climate models. *Bulletin of the American Meteorological Society*, *82*, 2797–2809. https://doi.org/10.1175/1520-0477(2001)082<2797:MRWUIH>2.3.CO;2

Feddes, R. A., Kowalik, P., Kolinska-Malinka, K., & Zaradny, H. (1976). Simulation of field water uptake by plants using a soil water dependent root extraction function. *Journal of Hydrology*, *31*, 13–26. https://doi.org/10.1016/0022-1694(76)90017-2

Feddes, R. A., Kowalik, P. J., & Zaradny, H. (1978). *Simulation of field water use and crop yield*. Wageningen, the Netherlands: Centre for Agricultural Publishing and Documentation.

Feng, S. Y., Jiang, J., Huo, Z. L., & Zhang, C. B. (2014). Optimization of irrigation scheduling under deficit irrigation with saline water for spring wheat based on SWAP model. *Nongye Gongcheng Xuebao (Beijing)*, *30*, 66–75.

Gao, H. B., & Shao, M. A. (2011). Effect of temperature on soil moisture parameters. *Advances in Water Science*, *22*, 484–494.

Goosheh, M., Pazira, E., Gholami, A., Andarzian, B., & Panahpour, E. (2018). Improving irrigation scheduling of wheat to increase water productivity in shallow groundwater conditions using Aquacrop. *Irrigation and Drainage*, *67*, 738–754. https://doi.org/10.1002/ird.2288

Green, S. R., & Clothier, B. E. (1995). Root water uptake by kiwifruit vines following partial wetting of the root zone. *Plant Soil*, *173*, 317–328. https://doi.org/10.1007/BF00011470

Guo, X. H., Sun, X. H., Ma, J. J., Lei, T., Zheng, L. J., & Wang, P. (2018). Simulation of the water dynamics and root water uptake of winter wheat in irrigation at different soil depths. *Water*, *10*, 1033–1049. https://doi.org/10.3390/w10081033

Han, H. H., Ren, Y. J., Gao, C., Yan, Z. X., & Li, Q. Q. (2017). Response of winter wheat grain yield and water use efficiency to deficit irrigation in the North China Plain. *Emirates Journal of Food and Agriculture*, *29*, 971–977.

Hassanli, M., Ebrahimian, H., Mohammadi, E., Rahimi, A., & Shokouhi, A. (2016). Simulating maize yields when irrigating with saline water, using the AquaCrop, SALTMED, and SWAP models. *Agricultural Water Management*, *176*, 91–99. https://doi.org/10.1016/j.agwat.2016.05.003

Hladni, N., Jocic, S., Mijic, A., Miklic, V., & Miladinovic, D. (2016). Correlation and path analysis of yield and yield components of confectionary sunflower. *Genetika*, *48*, 827–835. https://doi.org/10.2298/GENSR1603827H

Iqbal, M. A., Shen, Y., Stricevic, R., Pei, H., Sun, H., Amiri, E., … del-Rio, S. (2014). Evaluation of the FAO AquaCrop model for winter wheat on the North China Plain under deficit irrigation from field experiment to regional yield simulation. *Agricultural Water Management*, *135*, 61–72. https://doi.org/10.1016/j.agwat.2013.12.012

Javaux, M., Schröder, T., Vanderborght, J., & Vereecken, H. (2008). Use of a three-dimensional detailed modeling approach for predicting root water uptake. *Vadose Zone Journal*, *7*, 1079, https://doi.org/10.2136/vzj2007.0115

Jha, S. K., Gao, Y., Liu, H., Huang, Z. D., Wang, G. S., Liang, Y. P., & Duan, A. W. (2017). Root development and water uptake in winter wheat under different irrigation methods and scheduling for North China. *Agricultural Water Management*, *182*, 139–150. https://doi.org/10.1016/j.agwat.2016.12.015

Jiang, J., Feng, S. Y., Ma, J. J., Huo, Z. L., & Zhang, C. B. (2016). Irrigation management for spring maize grown on saline soil based on SWAP model. *Field Crops Research*, *196*, 85–97. https://doi.org/10.1016/j.fcr.2016.06.011

Kramer, P. J. (1950). Effects of wilting on the subsequent intake of water by plants. *American Journal of Botany*, *37*, 280–284. https://doi.org/10.1002/j.1537-2197.1950.tb12195.x

Kroes, J. G., van Dam, J. C., Bartholomeus, R. P., Groenendijk, P., Heinen, M., Hendriks, R. F. A., … van Walsum, P. E. V. (2017). *SWAP version 4: Theory description and user manual*. Wageningen, the Netherlands: Wageningen Environmental Research. https://doi.org/10.18174/416321

Kumar, R., Shankar, V., & Jat, M. K. (2014). Evaluation of root water uptake models– A review. *ISH Journal of Hydraulic Engineering*, *21*, 115–124. https://doi.org/10.1080/09715010.2014.981955

Li, C. X., Zhou, X. G., Sun, J. S., Wang, H. Z., & Gao, Y. (2014). Dynamics of root water uptake and water use efficiency under alternate partial root-zone irrigation. *Desalination Water Treat*, *52*, 2805–2810. https://doi.org/10.1080/19443994.2013.822647

Li, Q. Q., Bian, C. Y., Liu, X. H., Ma, C. J., & Liu, Q. R. (2015). Winter wheat grain yield and water use efficiency in wide-precision planting pattern under deficit irrigation in North China Plain. *Agricultural Water Management*, *153*, 71–76. https://doi.org/10.1016/j.agwat.2015.02.004

Li, S., Zhao, X. J., Xie, Y., Zhai, J. R., Liu, G., Gao, X. F., … Gao, Y. (2018). Parameter estimation of soil water retention curve based on soil physical and chemical properties of Van Genuchten model. *Dili Kexue*, *38*, 1189–1197. https://doi.org/10.13249/j.cnki.sgs.2018.07.021

Ma, Y., Feng, S. Y., & Song, X. F. (2015). Evaluation of optimal irrigation scheduling and groundwater recharge at representative sites in the North China Plain with SWAP model and field experiments. *Computers and Electronics in Agriculture*, *116*, 125–136. https://doi.org/10.1016/j.compag.2015.06.015

Martínez-Ferri, E., Muriel-Fernández, J. L., & Díaz, J. A. R. (2013). Soil water balance modelling using SWAP. *Outlook on Agriculture*, *42*, 93–102. https://doi.org/10.5367/oa.2013.0125

McCully, M. E., & Boyer, J. S. (1997). The expansion of maize root-cap mucilage during hydration. 3. Changes in water potential and water content. *Physiologia Plantarum*, *99*, 169–177. https://doi.org/10.1111/j.1399-3054.1997.tb03445.x

Mkhabela, M. S., & Bullock, P. R. (2012). Performance of the FAO AquaCrop model for wheat grain yield and soil moisture simulation in Western Canada. *Agricultural Water Management*, *110*, 16–24. https://doi.org/10.1016/j.agwat.2012.03.009

Mokhtari, A., Noory, H., & Vazifedoust, M. (2018). Improving crop yield estimation by assimilating LAI and inputting satellite-based surface incoming solar radiation into SWAP model. *Agricultural and Forest Meteorology*, *250–251*, 159–170. https://doi.org/10.1016/j.agrformet.2017.12.250

Moradi, A. B., Carminati, A., Lamparter, A., Woche, S. K., Bachmann, J., Vetterlein, D., … Oswald, S. E. (2012). Is the rhizosphere temporarily water repellent? *Vadose Zone Journal*, *11*, https://doi.org/10.2136/vzj2011.0120

Mostafazadeh-Fard, B., Mansouri, H., Mousavi, S. F., & Feizi, M. (2007). Application of the SWAP model for sustainable agriculture in an arid region. *Ecosytems and Sustainable Development*, *6*, 407–415. https://doi.org/10.2495/ECO070381

Nobel, P. S., & Huang, B. (1992). Hydraulic and structural changes for lateral roots of two desert succulents in response to soil drying and rewetting. *International Journal of Plant Sciences*, *153*, 163–170. https://doi.org/10.1086/297073

Nulsen, R. A., & Thurtell, G. W. (1978). Recovery of corn leaf water potential after severe water stress. *Agronomy Journal*, *70*, 903–906. https://doi.org/10.2134/agronj1978.00021962007000060003x

Prasad, R. (1988). A linear root water uptake model. *Journal of Hydrology*, *99*, 297–306. https://doi.org/10.1016/0022-1694(88)90055-8

Rallo, G., Agnese, C., Minacapilli, M., & Provenzano, G. (2012). Comparison of SWAP and FAO agro-hydrological models to schedule irrigation of wine grapes. *Journal of Irrigation and Drainage Engineering*, *138*, 581–591. https://doi.org/10.1061/(ASCE)IR.1943-4774.0000435

Richards, L. A. (1931). Capillary conduction of liquids through porous mediums. *Physics*, *1*, 318–333. https://doi.org/10.1063/1.1745010

Salemi, H., Soom, M. A. M., Lee, T. S., Mousavi, S. F., Ganji, A., & Yusoff, M. K. (2011). Application of AquaCrop model in deficit irrigation management of winter wheat in arid region.

African Journal of Agricultural Research, *610*, 2204–2215. https://doi.org/10.5897/ajar10.1009

Seker, H., & Serin, Y. (2004). Explanation of the relationships between seed yield and some morphological traits in smooth bromegrass (Bromus inermis Leyss.) by path analysis. *European Journal of Agronomy*, *21*, 1–6. https://doi.org/10.1016/S1161-0301(03)00055-8

Šimůnek, J., & Hopmans, J. W. (2009). Modeling compensated root water and nutrient uptake. *Ecological Modelling*, *220*, 505–521. https://doi.org/10.1016/j.ecolmodel.2008.11.004

Sonkar, I., Kaushika, G. S., & Hari Prasad, K. S. (2018). Modeling moisture flow in root zone: Identification of soil hydraulic and root water uptake parameters. *Journal of Irrigation and Drainage Engineering*, *144*, 04018029. https://doi.org/10.1061/(ASCE)IR.1943-4774.0001342

Steduto, P., Hsiao, T. C., Raes, D., & Fereres, E. (2009). AquaCrop-the FAO crop model to simulate yield response to water: I. Concepts and underlying principles. *Agronomy Journal*, *101*, 426–437. https://doi.org/10.2134/agronj2008.0139s

Tang, J. J., Folmer, H., & Xue, J. H. (2015). Technical and allocative efficiency of irrigation water use in the Guanzhong Plain, China. *Food Policy*, *50*, 43–52. https://doi.org/10.1016/j.foodpol.2014.10.008

Tang, J. J., Folmer, H., & Xue, J. H. (2016). Adoption of farm-based irrigation water-saving techniques in the Guanzhong Plain, China. *Agricultural Economics*, *47*, 445–455. https://doi.org/10.1111/agec.12243

Toumi, J., Er-Raki, S., Ezzahar, J., Khabba, S., Jarlan, L., & Chehbouni, A. (2016). Performance assessment of AquaCrop model for estimating evapotranspiration, soil water content and grain yield of winter wheat in Tensift Al Haouz (Morocco): Application to irrigation management. *Agricultural Water Management*, *163*, 219–235. https://doi.org/10.1016/j.agwat.2015.09.007

Van Genuchten, M. T., Leij, F. J., Yates, S. R., & Williams, J. R. (1991). *The RETC code for quantifying the hydraulic functions of unsaturated soils*. Riverside, CA: USDA Aricultural Research Service, US Salinity Laboratory.

Vereecken, H., Schnepf, A., Hopmans, J. W., Javaux, M., Or, D., Roose, T., … Young, I. M. (2016). Modeling soil processes: Review, key challenges, and new perspectives. *Vadose Zone Journal*, *15*, 1–57. https://doi.org/10.2136/vzj2015.09.0131

Vrugt, J. A., Hopmans, J. W., & Simunek, J. (2001). Calibration of a two-dimensional root water uptake model. *Soil Science Society of America Journal*, *65*, 1027–1037. https://doi.org/10.2136/sssaj2001.6541027x

Wraith, J. M., Baker, J. M., & Blake, T. K. (1995). Water uptake resumption following soil drought: A comparison among four barley genotypes. *Journal of Experimental Botany*, *46*, 873–880. https://doi.org/10.1093/jxb/46.7.873

Wright, S. (1921). Systems of mating. I. The biometric relations between parent and offspring. *Genetics*, *6*, 111–123. https://doi.org/10.1007/bf02983038

Xue, Q., Zhu, Z., Musick, J. T., Stewart, B. A., & Dusek, D. A. (2003). Root growth and water uptake in winter wheat under deficit irrigation. *Plant Soil*, *257*, 151–161. https://doi.org/10.1023/A:1026230527597

Yang, D. J., Zhang, T. Q., Zhang, K. F., Greenwood, D. J., Hammond, J. P., & White, P. J. (2009). An easily implemented agro-hydrological procedure with dynamic root simulation for water transfer in the crop–soil system: Validation and application. *Journal of Hydrology*, *370*, 177–190. https://doi.org/10.1016/j.jhydrol.2009.03.005

Yao, Y. F., & Shao, M. A. (2015). Effect of measure time on soil saturated hydraulic conductivity by constant head method. *Chinese Journal Soil Science*, *46*, 327–333. https://doi.org/10.19336/j.cnki.trtb.2015.02.011

Yu, L., Zeng, Y., Su, Z., Cai, H., & Zheng, Z. (2016). The effect of different evapotranspiration methods on portraying soil water dynamics and ET partitioning in a semi-arid environment in Northwest China. *Hydrology and Earth System Sciences*, *20*, 975–990. https://doi.org/10.5194/hess-20-975-2016

Yu, L. Y., Cai, H. J., Zheng, Z., Li, Z. J., & Wang, J. (2017). Towards a more flexible representation of water stress effects in the nonlinear Jarvis model. *Journal of Integrative Agriculture*, *16*, 210–220. https://doi.org/10.1016/S2095-3119(15)61307-7

Zarebanadkouki, M., Ahmed, M., Hedwig, C., Benard, P., Kostka, S. J., Kastner, A., & Carminati, A. (2018). Rhizosphere hydrophobicity limits root water uptake after drying and subsequent rewetting. *Plant Soil*, *428*, 265–277. https://doi.org/10.1007/s11104-018-3677-7

Zarebanadkouki, M., Ahmed, M. A., & Carminati, A. (2016). Hydraulic conductivity of the root-soil interface of lupin in sandy soil after drying and rewetting. *Plant Soil*, *398*, 267–280. https://doi.org/10.1007/s11104-015-2668-1

Zeng, W. Z., Lei, G. Q., Zha, Y. Y., Fang, Y. H., Wu, J. W., & Huang, J. S. (2018). Sensitivity and uncertainty analysis of the HYDRUS-1D model for root water uptake in saline soils. *Crop and Pasture Science*, *69*, 163, https://doi.org/10.1071/CP17020

Zhang, X. Y., Pei, D., & Chen, S. Y. (2004). Root growth and soil water utilization of winter wheat in the North China Plain. *Hydrological Processes*, *18*, 2275–2287. https://doi.org/10.1002/hyp.5533

Zheng, Z., Cai, H. J., Hoogenboom, G., Chaves, B., & Yu, L. Y. (2016). Limited irrigation for improving water use efficiency of winter wheat in the Guanzhong Plain of Northwest China. *Transactions of the ASABE*, *59*, 1841–1852. https://doi.org/10.13031/trans.59.11810

How to cite this article: Wang X, Cai H, Zheng Z, Yu L, Wang Z, Li L. Modelling root water uptake under deficit irrigation and rewetting in Northwest China. *Agronomy Journal*. 2020;112:158–174. https://doi.org/10.1002/agj2.20043